JOURNAL OF SOLID STATE CHEMISTRY **134,** 38–44 (1997)
ARTICLE NO. SC977532

Phase Equilibria in the La–Sr–Mn–O System

V. A. Cherepanov,[1] L. Yu. Barkhatova, and V. I. Voronin*

*Department of Chemistry, Ural State University, 51 Lenin av., Ekaterinburg, 620083, Russia, and *Institute for Metal Physics, Ural Branch of RAS, 18 S. Kovalevskaya st., Ekaterinburg, GSP-170, 620219, Russia*

Received April 21, 1997; accepted June 30, 1997

Based on the results of X-ray diffraction analysis of quenched samples and coulometric titration measurements, the phase equilibria of the La–Sr–Mn–O system at 1100°C were examined and are illustrated in the form of phase diagrams. Two types of solid solutions $La_{1-x}Sr_xMnO_{3\pm y}$ and $(La_{1-x}Sr_x)_2MnO_{4\pm\lambda}$ were found to exist in the system. The homogeneity ranges of solid solutions depended on thermodynamic conditions (T, P_{O_2}, and composition of the system).

INTRODUCTION

Recently there has arisen great interest in the alkali earth-substituted lanthanum manganates because of their electrical, catalytic, and mechanical properties, which make them useful as cathodes in fuel cells, catalysts, oxygen membranes, and other items (1, 2). The effect of the giant magnetoresistance found in these systems has also drawn attention to them (3). Thus, a knowledge of phase equilibria in the La–Sr–Mn–O system at different temperatures and oxygen partial pressures in very important. Related quasibinary systems have more or less been studied before.

La–Mn–O system. Two complex oxides, $LaMnO_{3\pm\delta}$ and $La_2MnO_{4+\delta}$, exist in this system. Only $LaMnO_{3+\delta}$ appears to be stable in air. The phase diagram of the system in air was constructed by van Roosmalen *et al.* (4). $La_2MnO_{4.15}$ was obtained in atmosphere with low oxygen pressure at temperatures higher than 1380°C (5). The thermodynamic stability of $LaMnO_{3+\delta}$ had been studied by TGA (6, 7), gas chromatography (8), EMF technique (9), and electrical conductivity measurements (10). It had been shown that lanthanum manganate decomposes to MnO and La_2O_3 below 1380°C. The oxygen content of $LaMnO_{3\pm\delta}$ changes from an oxygen excess in air to an oxygen deficit near the decomposition boundary (5–7, 10–14). The oxygen content of lanthanum manganate is closely connected to the oxidation state of manganese ions. The correlation between crystal structure and Mn^{4+} content had been described elsewhere (15–17). Together with oxygen nonstoichiometry, cation nonstoichiometry was observed for lanthanum manganate. A deficit of lanthanum $La_{1-y}MnO_{3+\delta}$ was reported in (4, 13, 18–20) and a deficit of manganese in (4). The phase boundary on the La-rich side depends on temperature. It changes from $\xi_{Mn} = n_{Mn}/(n_{Mn} + n_{La}) = 0.452$ at 900°C to $\xi_{Mn} = 0.475$ at 1200°C. The phase boundary on the Mn-rich side maintained a practically constant composition $\xi_{Mn} = 0.524$ with increasing temperature to 1700°C (4).

Sr–Mn–O system. A number of phases were found to be stable in air in the temperature range 800–1800°C, i.e., $SrMn_3O_z$, $SrMnO_3$, Sr_2MnO_4, $SrMn_2O_7$, and $Sr_4Mn_3O_{10}$; however, the phase diagram of this system had not been constructed earlier.

$SrMn_3O_z$ has orthorhombic structure with unit cell parameters $a = 9.45$, $b = 11.51$, and $c = 5.05$ Å (21). The oxygen content (x) changes from 6.06 at 900°C to 5.78 at 1200°C. At 1215°C, $SrMn_3O_z$ decomposes on Mn_3O_4 and $SrMnO_3$.

α-$SrMnO_3$ has a hexagonal structure (22–24). Above 1036°C α-$SrMnO_3$ begins to lose oxygen, and at 1400°C, its composition can be expressed as $SrMnO_{2.89}$ with a distorted hexagonal structure.

The crystal structure of α-Sr_2MnO_4, which is formed in air in the temperature range 800–1200°C, has not been described. At higher temperatures, α forms of $SrMnO_3$ and Sr_2MnO_4 are transformed into β-forms. β-Sr_2MnO_4 has a tetragonal K_2NiF_4-type structure ($a = 3.787$ Å, $c = 12.497$ Å) (25). The perovskite-type β-$SrMnO_{3-x}$ was obtained in air in the temperature range ~1200–1400°C. The value of x changes from 0.26 to 0.38 (24). It melts incongruently at 1740°C.

$Sr_3Mn_2O_7$ appears at 1700°C and remains the only stable phase at 1800°C (26).

Single crystals of $Sr_4Mn_3O_{10}$ were grown from a melted mixture of components with $SrCl_2$–SrF_2 as a solvent (33). It has an orthorhombic structure with the unit cell parameters $a = 5.443$, $b = 12.427$, and $c = 12.500$ Å. Above 1500°C, it decomposes.

[1]To whom correspondence should be addressed.

0022-4596/97 $25.00

La–Sr–O system. It has been shown (27) that no ternary oxides exist in the La–Sr–O system at 1100°C in air, but SrO is slightly soluble in La_2O_3 [$\xi_{Sr} = n_{Sr}/(n_{Sr} + n_{La}) \leq 0.05$]. All ternary oxides found in this system existed at temperatures above 1500°C (28).

La–Sr–Mn–O system. Solid solutions with perovskite-type structure, $La_{1-x}Sr_xMnO_{3\pm\delta}$, have been recognized since Jonker (29). He obtained $La_{1-x}Sr_xMnO_{3\pm\delta}$ with $x \leq 0.7$ by the standard ceramic technique in air in the temperature range 1200–1400°C. Lauret *et al.* (30) obtained the solid solution $La_{1-x}Sr_xMnO_{3\pm\delta}$ with $x = 0.8$. It was shown (30, 31) that all compositions had rhombohedral (hexagonal) structure ($R\bar{3}c$ space group).

The thermodynamic stability of $La_{1-x}Sr_xMnO_{3\pm\delta}$ with $x = 0.2$ and 0.4 at low oxygen pressure has been studied by Mizuzaki *et al.* (32) by the coulometric titration technique. They found that $La_{0.8}Sr_{0.2}MnO_{3-\delta}$ at low oxygen pressure decomposes on La_2O_3, MnO, and $La_{2-x}Sr_xMnO_4$, whereas $La_{0.6}Sr_{0.4}MnO_{3-\delta}$ decomposes on $(La_{0.6}Sr_{0.4})_2MnO_4$ and MnO. These data do not agree with the results of Kuo *et al.* (11), who reported that the decomposition products of $La_{0.8}Sr_{0.2}MnO_{3-\delta}$ are La_2O_3, MnO, $SrMnO_3$, and La_2MnO_4. Exact values of the equilibrium decomposition pressure were not cited in either paper; however, approximate values taken from the figures are for $La_{0.8}Sr_{0.2}MnO_{3-\delta}$, about 10^{-16} atm at 900°C (32) or 10^{-14} atm at 1100°C (11), and for $La_{0.6}Sr_{0.4}MnO_{3-\delta}$, about 10^{-11} atm.

The possibility of cation nonstoichiometry in strontium-doped lanthanum manganates that can be described by the formula $(La_{1-x}Sr_x)_{1-y}MnO_{3\pm\delta}$ in air in the temperature range 800–1200°C has been reported (19). The value of y decreased from 0.15 to 0 with an increase in strontium content (x) from 0 to 0.4. It should be noted that from the structural point of view, there were three single phases with different structures (two orthorhombic and rhombohedral) inside the homogeneity range.

Solid solutions of the general formula $(La_{1-x}Sr_x)_2MnO_4$ were obtained as decomposition products of $La_{1-x}Sr_xMnO_{3\pm\delta}$ in an inert atmosphere (32) and by solid-state synthesis with $x = 0.5$ (34) and $0.5 \leq x \leq 1$ in (35). All solid solutions had tetragonal K_2NiF_4-type structure. Thermodynamic data for these solid solutions have not been found in the literature.

Thus, despite the wealth of information on the physicochemical properties of the single phases found in the La–Sr–Mn–O system, the phase diagram and thermodynamic properties of the phases are still not clear. Therefore, the aim of the present work was determination of the phase relations as a function of temperature and oxygen pressure and construction of the phase diagram of the La–Sr–Mn–O system.

EXPERIMENTAL

The starting materials were La_2O_3 (99.99% purity), Mn_2O_3 of "pure for analysis" grade, and $SrCO_3$ of "special purity" grade, previously annealed in air at 1200°C (La_2O_3) and 700°C (Mn_2O_3 and $SrCO_3$) for 3–5 h. The materials were mixed in appropriate ratios and ground in an agate mortar. All samples were fired in air at 850°C for 24 h. 950°C for 24 h, and 1100°C for 24–70 h. A number of samples were fired later at 1100°C in atmospheres with different oxygen partial pressures for 24–40 h. Oxygen pressure was monitored and controlled with the help of zirconia ($ZrO_2 + 0.1Y_2O_3$) cells. X-ray diffraction (XRD) patterns of powder samples were obtained on a DRON-3 diffractometer using Cu$K\alpha$ radiation. Neutron diffraction measurements were made at the research reactor located near Ekaterinburg, Russia, on the D7A diffractometer with a double monochromator (002) reflection of a single crystal of pyrolytic graphic and a (333) reflection of germanium. The wavelength employed was 1.515 Å. The boundary of phase stability of $La_{0.7}Sr_{0.3}MnO_{3-\delta}$ was determined using coulometric titration with solid zirconia-based electrolyte.

Because oxygen content and oxidation state of manganese ions change as a function of metal ratio and oxygen pressure, the composition in the phase diagrams was presented as the relative mole fraction of metal $\xi_i = n_i/\sum n_i$, for example, $\xi_{Mn} = n_{Mn}/(n_{La} + n_{Sr} + n_{Mn})$ in the quasiternary La–Sr–Mn–O system and $\xi_{Mn} = n_{Mn}/(n_{Sr} + n_{Mn})$ in the quasibinary Sr–Mn–O system (n = amount of moles of corresponding metal component). The oxygen content of solid phases was not taken into account in the phase diagrams. This simplified the graphic presentation of the phase diagrams.

RESULTS AND DISCUSSION

Phase Equilibria at 1100°C in Air

The only phases that have been found to exist at 1100°C in air in quasibinary systems were $LaMnO_{3+\delta}$ in the La–Mn–O system and $SrMn_3O_z$, α-$SrMnO_3$, and α-Sr_2MnO_4 in the Sr–Mn–O system. The slight solubility of SrO in La_2O_3 ($\xi_{Sr} \approx 0.05$) in the La–Sr–O system was reported earlier (27).

The only phase found in the quasiternary La–Sr–Mn–O system was a solid solution based on $LaMnO_{3+\delta}$. Based on XRD analysis samples with $La_{1-x}Sr_xMnO_{3+\delta}$ composition ($x = 0.1$, 0.2, and 0.3) were identified as single phases. The sample with $x = 0.4$ consisted of Sr-saturated $La_{1-x}Sr_xMnO_{3+\delta}$ and α-$SrMnO_3$. The composition of the Sr-saturated solid solution was estimated to be $La_{0.62}Sr_{0.38}MnO_{3+\delta'}$ by quantitative XRD analysis, where δ' is the fixed (positive or negative) value of oxygen nonstoichiometry at 1100°C in air for a fixed value of $x \approx 0.38$.

The solid solution $La_{0.9}Sr_{0.1}MnO_{3+y}$ quenched from 1100°C in air had orthorhombic structure (*Pnma* space group), similar to $LaMnO_{3+\delta}$. Solid solutions with $x = 0.2$ and 0.3 quenched from 1100°C in air had rhombohedral structure $R\bar{3}c$ space group). α-$SrMnO_3$, which was present in all samples of nominal composition $La_{1-x}Sr_xMnO_{3+\delta}$ ($x \geq 4$) had hexagonal structure ($P6_3/mmc$ space group). The unit cell parameters calculated in the present work and listed in Table 1 are in good agreement with those obtained in (15, 24, 31).

The homogeneity range of $La_{1-x}Sr_xMnO_{3+\delta}$ in the direction of Mn-rich and Mn-deficient compositions to form solid solutions such as $La_{1-x}Sr_xMn_{1\pm y}O_{3+\delta}$ has not been examined in this work.

The results of XRD patterns of more than 40 samples of different composition allowed us to divide the phase triangle as shown in Fig. 1. Special attention has been paid to the possibility of formation of $Sr_{2-x}La_xMnO_4$ solid solution in air at 1100°C. It was found that the sample with nominal composition $Sr_{1.96}La_{0.04}MnO_4$ quenched from 1100°C consisted of Sr_2MnO_4, $La_{0.62}Sr_{0.38}MnO_{3+\delta}$, and La_2O_3(SrO) solid solution. Thus, we concluded that the solubility of La ions in Sr_2MnO_4 was negligible under these conditions and did not exceed $x = 0.04$. The homogeneity range of perovskite-type solid solution in the direction of Mn-rich and Mn-deficient compositions was drawn based on the results taken from (4, 19).

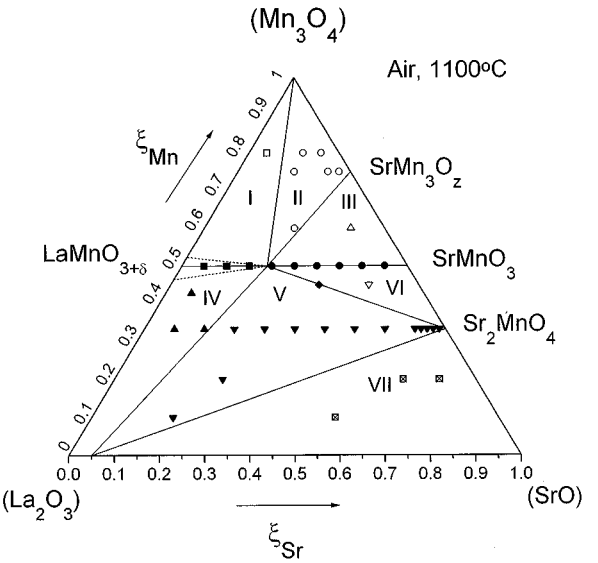

FIG. 1. Gibbs triangle of quasiternary La–Sr–Mn–O system at 1100°C in air. The fields inside the triangle represent the following coexisting phases: (I) $La_{1-x}Sr_xMnO_{3+\delta} + Mn_3O_4$; (II) $La_{0.62}Sr_{0.38}MnO_{3\pm\delta} + Mn_3O_4 + SrMn_3O_z$; (III) $La_{0.62}Sr_{0.38}MnO_{3\pm\delta} + SrMn_3O_z + SrMnO_3$; (IV) $La_{1-x}Sr_xMnO_{3\pm\delta} + La_2O_3 -$ SrO solid solution; (V) $La_{0.62}Sr_{0.38}MnO_{3\pm\delta} + Sr_2MnO_4$ + Sr-saturated La_2O_3–SrO solid solution; (VI) $La_{0.62}Sr_{0.38}MnO_{3\pm\delta} + Sr_2MnO_4 + SrMnO_3$; (VII) Sr_2MnO_4 + Sr-saturated La_2O_3–SrO solid solution + SrO.

Phase Equilibria at 1100°C and Various Oxygen Pressures

The study of phase equilibria at 1100°C and various oxygen partial pressures [$0.21 \geq P_{O_2}$ (atm) $\geq 10^{-14}$] within the compositional ranges $(n_{La} + n_{Sr})/n_{Mn} = 1$ and $(n_{La} + n_{Sr})/n_{Mn} = 2$ was performed by XRD of quenched samples. The samples, previously equilibrated in air, were annealed in the special cell at 1100°C and fixed oxygen pressure and then quenched to room temperature by replacing them inside the evacuated cell from the hot side of the cell to the cooled metal vessel.

With respect to the phase triangle shown in Fig. 1 the observed phase equilibria can be represented as cross sections perpendicular to the plane of the triangle along the lines ⟪$LaMnO_{3+\delta}$–$SrMnO_3$⟫ and ⟪"La_2MnO_4"–Sr_2MnO_4⟫, respectively. The results obtained in such cross sections are shown in Figs. 2 and 3.

The changes in the limiting composition of $La_{1-x}Sr_xMnO_{3\pm y}$ versus oxygen partial pressure (Fig. 2) is rather unusual. In the oxygen pressure range 0.21–10^{-9} atm the limiting value of x increases from ~ 0.38 to ~ 0.7, whereas oxygen pressure decreases. Further decrease in oxygen pressure led to a decrease in strontium content in the

TABLE 1
Unit Cell Parameters of $La_{1-x}Sr_xMnO_{3+\delta}$ Quenched from 1100°C in Air

Total value of x	Phase composition	Unit cell parameters (Å)			Space group
		a	b	c	
0.0	$LaMnO_{3+\delta}$	5.5292(2)	7.7824(2)	5.5391(2)	*Pnma*
0.1	$La_{0.9}Sr_{0.1}MnO_{3\pm\delta}$	5.4995(2)	7.7900(3)	5.5405(2)	*Pnma*
0.2	$La_{0.8}Sr_{0.2}MnO_{3\pm\delta}$	5.5282(1)		13.3683(2)	$R\bar{3}c$
0.3	$La_{0.7}Sr_{0.3}MnO_{3\pm\delta}$	5.5073(1)		13.3571(3)	$R\bar{3}c$
0.4	$La_{0.62}Sr_{0.38}MnO_{3\pm\delta} + SrMnO_3$	5.4958(1)		13.3685(4)	$R\bar{3}c$
		5.4483(5)		9.0746(9)	$P6_3/mmc$
1.0	$SrMnO_3$	5.4483(3)		9.0746(5)	$P6_3/mmc$

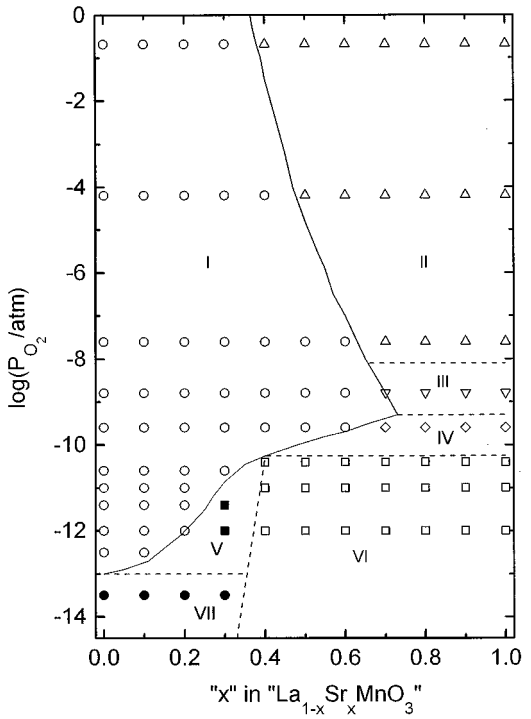

FIG. 2. "Oxygen pressure–composition" cross section of the phase diagram of the system La–Sr–Mn–O along the line ⟪$LaMnO_{3+\delta}$–$SrMnO_3$⟫ at 1100°C. The fields represent the following coexisting phases: (I) $La_{1-x}Sr_xMnO_{3\pm\delta}$ single phase; (II) Sr-saturated $La_{1-x}Sr_xMnO_{3\pm\delta}$ + α-$SrMnO_3$; (III) Sr-saturated $La_{1-x}Sr_xMnO_{3\pm\delta}$ + β-$SrMnO_3$; (IV) Sr-saturated $La_{1-x}Sr_xMnO_{3\pm\delta}$ + β-$SrMnO_3$; (V) Sr-saturated $La_{1-x}Sr_xMnO_{3\pm\delta}$ + La-saturated $(La_{1-x}Sr_x)_2MnO_{4\pm\lambda}$ + Sr-saturated La_2O_3–SrO solid solution; (VI) $(La_{1-x}Sr_x)_2MnO_{4\pm\lambda}$ + MnO; (VII) La-saturated $(La_{1-x}Sr_x)_2MnO_{4\pm\lambda}$ + Sr-saturated La_2O_3–SrO solid solution + MnO.

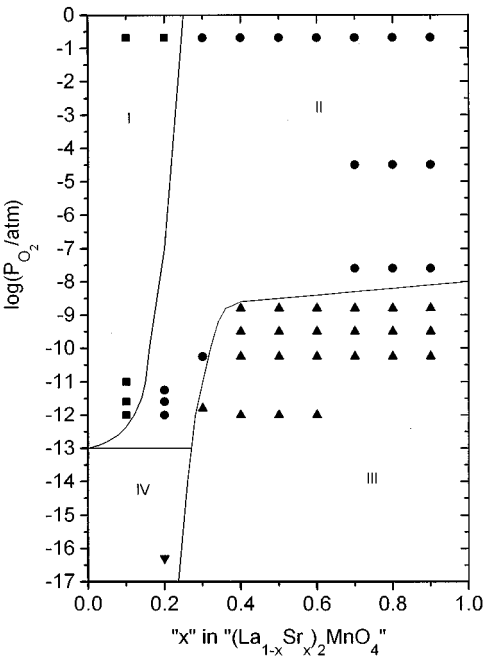

FIG. 3. "Oxygen pressure–composition" cross section of the phase diagram of the system La–Sr–Mn–O along the line ⟪"La_2MnO_4"–$SrMnO_3$⟫ at 1100°C. The fields represent the following coexisting phases: (I) $La_{1-x}Sr_xMnO_{3\pm\delta}$ + La_2O_3–SrO solid solution; (II) Sr-saturated $La_{1-x}Sr_xMnO_{3\pm\delta}$ + Sr-saturated La_2O_3–SrO solid solution + Sr_2MnO_4; (III) $(La_{1-x}Sr_x)_2MnO_{4\pm\lambda}$ single phase; (IV) La-saturated $(La_{1-x}Sr_x)_2MnO_{4\pm\lambda}$ + Sr-saturated La_2O_3–SrO solid solution + MnO.

Sr-saturated solid solution ($La_{1-x}Sr_xMnO^{sat}_{3\pm\delta}$). From the general point of view, it is obvious that the decrease in oxygen partial pressure must lead to a decrease in oxygen content in complex oxides and to a decrease in the average oxidation state of manganese ions. In contrast, the increase in Sr content leads to an increase in the average oxidation state of manganese ions and a decrease in oxygen content. Thus, the broadening of the homogeneity range of $La_{1-x}Sr_xMnO_{3\pm\delta}$ in the oxygen pressure range 0.21–10^{-9} atm can be explained as follows. Significant loss f oxygen inside that oxygen pressure range leads to a situation where, even if the average oxidation state of manganese ions decreases, the strontium content of the Sr-saturated sample can increase. In this way manganese ions reach their equilibrium average oxidation state, which became lower but at a slower rate in comparison with the changes in oxygen content. It was shown earlier that the thermodynamic properties of perovskites of 3d-transition metals strongly depend on their electronic configuration (36). So an equilibrium average oxidation state of manganese ions at fixed conditions (T, P_{O_2}, composition of the system) controls the composition of the solid solution. At lower oxygen pressure ($< 10^{-9}$ atm), when the losses of oxygen became much smaller, the decrease in the average oxidation state of manganese ions occurs mainly by a decrease in Sr content.

Decomposition of $LaMnO_3$ was found to occur inside the oxygen partial pressure range 10^{-13}–10^{-14} atm at 1100°C. This result is in good agreement with the value of equilibrium oxygen pressure for $LaMnO_3$, $\log(P_{O_2}/\text{atm}) = -13.25$, obtained by Borlera and Abbattista (5).

The value of the decomposition oxygen pressure of $La_{0.6}Sr_{0.4}MnO_{3\pm y}$, $\log(P_{O_2}/\text{atm}) = -10.25$, is in good agreement with that found in (32). This composition is also interesting because a change in the mechanism of the decomposition reaction of $La_{1-x}Sr_xMnO_{3\pm y}$ took place in the vicinity of $La_{0.6}Sr_{0.4}MnO_{3\pm y}$ as P_{O_2} decreased. The samples of $La_{1-x}Sr_xMnO_{3\pm y}$ with $0.7 > x > 0.4$ decomposed in the oxygen pressure range $\sim 10^{-9}$–$10^{-10.25}$ atm while oxygen pressure decreased according to the reaction

$$La_{1-x}Sr_xMnO^{(sat)}_{3\pm\delta} = \frac{1-x}{1-x'}La_{1-x'}Sr_{x'}MnO^{(sat')}_{3\pm\delta'} + \frac{x-x'}{2(1-x')}Sr_2Mn_2O_{5\pm z} + kO_2, \quad [1]$$

where $x' < x$. In this range of oxygen pressure, the samples whose compositions lie outside the homogeneity range of $La_{1-x}Sr_xMnO_{3\pm y}$ consist of solid solution with the limiting composition coexisting with $Sr_2Mn_2O_{5\pm z}$.

For oxygen pressures lower than $\sim 10^{-10.25}$ atm, the decomposition process can be written as follows:

$$La_{1-x}Sr_xMnO_{3\pm\delta}^{(sat)} = nLa_{1-x'}Sr_{x'}MnO_{3\pm\delta'}^{(sat')} + m(La_{1-y}Sr_y)_2MnO_{4\pm\lambda}^{(sat)} + (1-n-m)MnO + kO_2. \quad [2]$$

Here, $x > x'$ and $x < y$.

It should be noted that use of "equilibrium" EMF measurements in their standard form for determination of the phase boundary of $La_{1-x}Sr_xMnO_{3\pm\delta}^{(sat)}$ is debatable because reactions [1] and [2] do not represent true thermodynamic equilibria where all participants of the reactions coexist under the same conditions. In fact, the right sides of these reactions represent an equilibrium state at higher P_{O_2}, and the left sides, an equilibrium state at lower P_{O_2}. In this respect, the products of decomposition depend on the final P_{O_2}. As will be shown later, the products of decomposition of $La_{0.8}Sr_{0.2}MnO_{3-\delta}$ can be La_2O_3, MnO and $La_{2-x}Sr_x$ MnO_4, as was reported in (32), if the decrease in P_{O_2} that led to the decomposition was large enough and the final P_{O_2} was below the decomposition pressure of $LaMnO_3$. However, if the decrease in P_{O_2} is infinitely small, decomposition of $La_{0.8}Sr_{0.2}MnO_{3-\delta}$, we believe, must be described by reaction [2]. Nevertheless, the values of the stability boundaries determined by electrochemical removal of oxygen from the zirconia cell in (32) for $x = 0.2$ and 0.4 and in the present work for $x = 0.3$ are in good agreement with the results of XRD for quenched samples (Fig. 4).

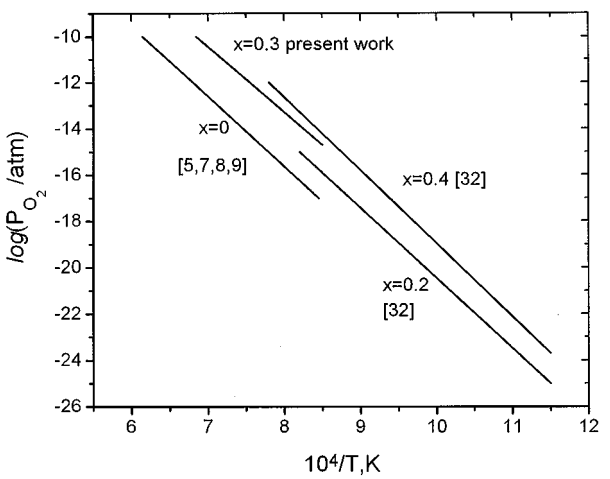

FIG. 4. Dissociation oxygen pressure of $La_{1-x}Sr_xMnO_{3\pm\delta}$ versus temperature.

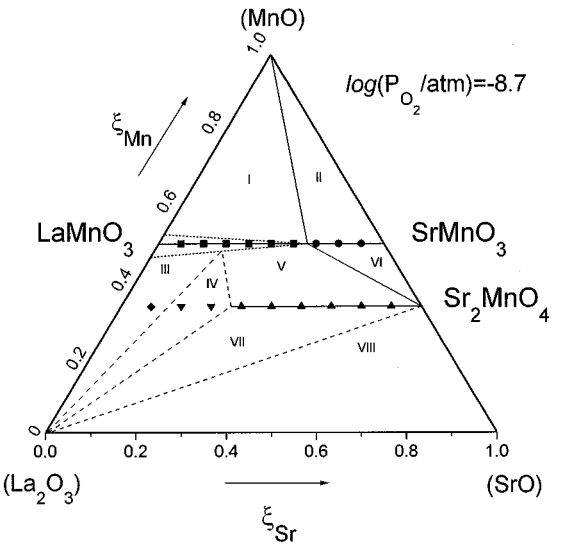

FIG. 5. Gibbs triangle of quasiternary La–Sr–Mn–O system at 1100°C and $P_{O_2} = 10^{-8.7}$ atm. The fields inside the triangle represent the following coexisting phases: (I) $La_{1-x}Sr_xMnO_{3\pm\delta}$ + MnO; (II) Sr-saturated $La_{1-x}Sr_xMnO_{3\pm\delta}$ + β-$SrMnO_3$ + MnO; (III) $La_{1-x}Sr_xMnO_{3\pm\delta}$ + La_2O_3–SrO solid solution; (IV) $La_{1-x}Sr_xMnO_{3\pm\delta}$ with some fixed x + La_2O_3–SrO solid solution of fixed concentration + La-saturated $(La_{1-x}Sr_x)_2MnO_{4\pm\lambda}$; (V) $La_{1-x}Sr_xMnO_{3\pm\delta}$ + $(La_{1+x}Sr_x)_2MnO_{4\pm\lambda}$; (VI) Sr-saturated $La_{1-x}Sr_xMnO_{3\pm\delta}$ + β-$SrMnO_3$ + Sr_2MnO_4; (VII) $(La_{1-x}Sr_x)_2MnO_{4\pm\lambda}$ + La_2O_3–SrO solid solution; (VIII) Sr-saturated La_2O_3–SrO solid solution + Sr_2MnO_4 + SrO.

$(La_{1-x}Sr_x)_2MnO_{4\pm\delta}$ solid solution was found to exist at 1100°C in atmospheres with $P_{O_2} \le 10^{-7}$ atm (Fig. 3). The homogeneity range of this solid solution broadens significantly in the P_{O_2} range $\approx 10^{-7}$–$10^{-8.5}$ atm and remains practically unchanged up to 10^{-14} atm. It is interesting that this broadening takes place approximately in the same range of P_{O_2} in which the homogeneity range of $La_{1-x}Sr_xMnO_{3\pm\delta}$ starts to narrow. It is known that $(La_{1-x}Sr_x)_2MnO_{4\pm\delta}$ solid solutions remain stable up to extremely low oxygen activities, even in an atmosphere of hydrogen (37).

The experimental results illustrated in Figs. 2 and 3 allow us to draw conjectural phase triangles at low oxygen partial pressures (Figs. 5–7). Although the possibility of cation nonstoichiometry has not been checked at low oxygen pressure in the present study, the homogeneity range of solid solution with the general formula $(La_{1-x}Sr_x)_{1\pm y}MnO_{3\pm\delta}$ is shown by the short-dash lines schematically, but omitted in the figure legends. Figure 7 represents an example of a final P_{O_2} at which the sample of nominal composition "$La_{0.8}Sr_{0.2}MnO_{3-\delta}$" consisted of La_2O_3, MnO, and $(La_{1-x}Sr_x)_2MnO_4$, as reported in (32).

CONCLUSION

It was shown that Sr content in Sr-saturated $La_{1-x}Sr_x$ $MnO_{3\pm\delta}^{(sat)}$ strongly depends on thermodynamic conditions

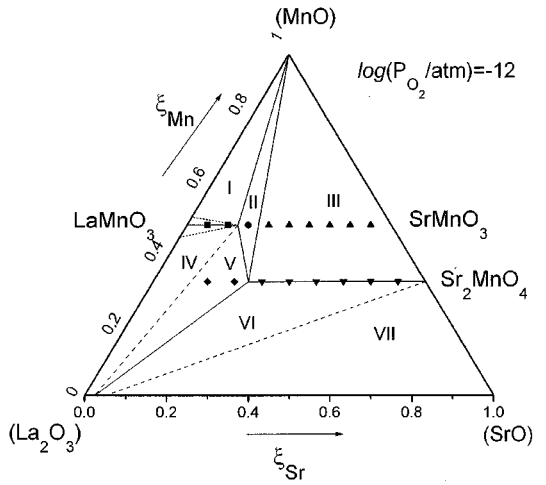

FIG. 6. Gibbs triangle of quasiternary La–Sr–Mn–O system at 1100°C and $P_{O_2} = 10^{-12}$ atm. The fields inside the triangle represent the following coexisting phases: (I) $La_{1-x}Sr_xMnO_{3\pm\delta}$ + MnO; (II) Sr-saturated $La_{1-x}Sr_xMnO_{3\pm\delta}$ + La-saturated $(La_{1-x}Sr_x)_2MnO_{4\pm\lambda}$ + MnO; (III) $(La_{1-x}Sr_x)_2MnO_{4\pm\lambda}$ + MnO; (IV) $La_{1-x}Sr_xMnO_{3\pm\delta}$ + La_2O_3–SrO solid solution; (V) Sr-saturated $La_{1-x}Sr_xMnO_{3\pm\delta}$ + La-saturated $(La_{1-x}Sr_x)_2MnO_{4\pm\lambda}$ + La_2O_3–SrO solid solution of fixed concentration; (VI) $(La_{1-x}Sr_x)_2MnO_{4\pm\lambda}$ + La_2O_3–SrO solid solution; (VII) Sr-saturated La_2O_3–SrO solid solution + Sr_2MnO_4 + SrO.

and is controlled mainly by the oxygen content and equilibrium advantageous average oxidation state of manganese ions. The mechanism of the decomposition reaction of $La_{1-x}Sr_xMnO_{3\pm\delta}^{(sat)}$ changed near $x \approx 0.4$ at $P_{O_2} \approx 10^{-10.25}$ atm. $(La_{1-x}Sr_x)_2MnO_{4\pm\delta}$ solid solution was found to exist at 1100°C and $P_{O_2} \leq 10^{-7}$ atm. The coexistence of the phases in samples of different composition are shown in cross sections of the phase diagram.

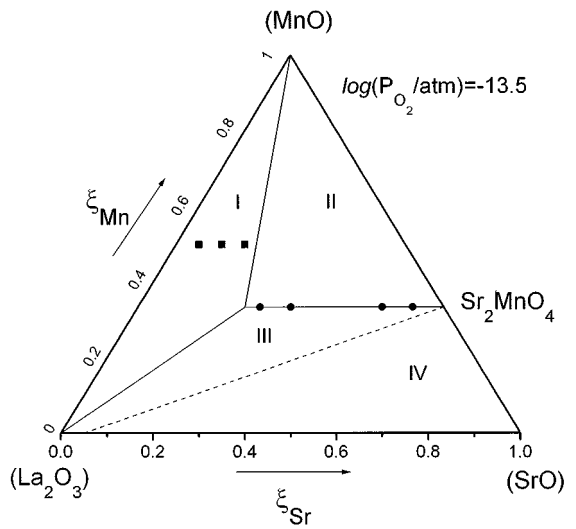

FIG. 7. Gibbs triangle of quasiternary La–Sr–Mn–O system at 1100°C and $P_{O_2} = 10^{-13.5}$ atm. The fields inside the triangle represent the following coexisting phases: (I) La-saturated $(La_{1-x}Sr_x)_2MnO_{4\pm\lambda}$ + La_2O_3 + MnO; (II) $(La_{1-x}Sr_x)_2MnO_{4\pm\lambda}$ + MnO; (III) $(La_{1-x}Sr_x)_2MnO_{4\pm\lambda}$ + La_2O_3–SrO solid solution; (IV) Sr-saturated La_2O_3–SrO solid solution + Sr_2MnO_4 + SrO.

ACKNOWLEDGMENTS

This work was partly supported by grants N97-03-33632a and N97-02-17315a from the Russian Basic Science Foundation and Russian State Scientific and Technical Program "Neutron Investigation of Matter" (NN 96-104 and 96-401).

REFERENCES

1. S. Carter, A. Selcuk, R. J. Chater, J. Kajda, J. A. Kilner, and B. C. H. Steele, *Solid State Ionics* **53/56,** 597 (1992).
2. T. Nitadori, S. Kurihara, and M. Misono, *J. Catal.* **98,** 221 (1986).
3. V. Caignaert, A. Maignan, and B. Raveau, *Solid State Commun.* **95,** 357 (1995).
4. J. A. M. van Roosmalen, P. van Vlaanderen, E. H. P. Cordfunke, W. L. IJdo, and D. J. W. IJdo, *J. Solid State Chem.* **114,** 516 (1995).
5. M. L. Borlera and F. Abbattista, *J. Less-Common Metals* **92,** 55 (1983).
6. T. Nakamura, G. Petzow, and L. J. Gauckler, *Mater. Res. Bull.* **14,** 649 (1979).
7. N. Kamegashira and Y. Miyazaki, *Mater. Chem. Phys.* **11,** 187 (1984).
8. Yu. P. Vorobjev, A. A. Iovlev, S. A. Leontjev, A. N. Menj, S. A. Prokudina, and Ya. S. Rubinchik, *Izv. Akad. Nauk SSSR Neorg. Mater.* **15,** 1449 (1979). [In Russian]
9. O. M. Sreedharan, R. Pankajavalli, and J. B. Gnanamoorthy, *High Temp. Sci.* **16,** 251 (1983).
10. N. Kamegashira, Y. Miyazaki, and Y. Hiyoshi, *Mater. Lett.* **2,** 194 (1984).
11. J. H. Kuo, H. U. Anderson, and D. M. Sparlin, *J. Solid State Chem.* **83,** 52 (1989).
12. J. A. M. van Roosmalen and E. H. P. Cordfunke, *J. Solid State Chem.* **110,** 109 (1994).
13. B. C. Tofield and W. R. Scott, *J. Solid State Chem.* **10,** 183 (1974).
14. K. Kamata, T. Nakajima, T. Hayashi, and T. Nakamura, *Mater. Res. Bull.* **13,** 49 (1978).
15. A. K. Bogush, V. I. Pavlov, and L. V. Balyko, *Cryst. Res. Technol.* **118,** 589 (1983).
16. M. Verelst, N. Rangavittal, C. N. R. Rao, and A. Rousset, *J. Solid State Chem.* **104,** 74 (1993).
17. J. A. M. van Roosmalen, E. H. P. Cordfunke, R. B. Helmholdt, and H. W. Zandbergen, *J. Solid State Chem.* **110,** 100 (1994).
18. J. Mizusaki, H. Tagawa, Y. Yonemura, H. Minamiue, and H. Nambu, *in* "Proceedings, Second International Symposium: Ionic and Mixed Conductor Ceramics, San Fransisco, May 1994", p. 402.
19. Y. Takeda, S. Nakai, T. Kojima, R. Kanno, N. Imanishi, G. Q. Shen, O. Yamamoto, M. Mori, C. Asakawa, and T. Abe, *Mater. Res. Bull.* **26,** 153 (1991).
20. S. Habekost, P. Norby, J. E. Jørgensen, and B. Lebech, *Acta. Chem. Scand.* **48,** 377(1994).
21. T. Negas, *J. Solid State Chem.* **7,** 85 (1970).
22. K. Kuroda, N. Ishizawa, N. Mizutani, and M. Kato, *J. Solid State Chem.* **38,** 297 (1981).
23. Y. Syono and S. Akimoto, *J. Phys. Soc. Japan* **26,** 994 (1969).
24. T. Negas and R. S. Roth, *J. Solid State Chem.* **1,** 409 (1970).
25. V. Balz and K. Plieth, *Z. Electrochem.* **6,** 545 (1955).
26. N. Mizutani, A. Kitazawa, N. Ohkuma, and M. Kato, *Kogyo Kagaki Zasshi* **73,** 1097 (1970).
27. V. A. Cherepanov, L. Yu. Barkhatova, A. N. Petrov, and V. I. Voronin, *in* "Proceedings, IVth International Symposium: Solid Oxide Fuel Cells, Yokohama, Japan, June 18–23, 1995," p. 434.

28. L. M. Lopato, V. N. Pavlikov, L. I. Lugin, *et al*., *Dokl. Akad. Nauk Ukr. SSR Ser. B* **8,** 713 (1971).
29. G. H. Jonker, *Physica* **22,** 707 (1956).
30. H. Lauret, E. Caignol, and A. Hammou, *in* "Proceedings, IInd International Symposium: Solid Oxide Fuel Cells, June 2–5, 1995," p. 429.
31. A. Hammouche, E. Siebert, and A. Hammou, *Mater. Res. Bull.* **24,** 367 (1989).
32. J. Mizuzaki, H. Tagawa, K. Haraya, and T. Sasamoto, *Solid State Ionics* **49,** 111 (1991).
33. J. Fabry, J. Hybler, Z. Jirak, *et al*., *J. Solid State Chem.* **73,** 520 (1988).
34. B. Lesniewska and A. Bombic, *Zeszyty Nauk. Akad. Gorniczo-Hutniczej Stanislawa Staszica Matemat. Fiz. Chem.* **60,** 7 (1983).
35. A. Benabad, A. Daoudi, R. Salmon, and G. Le Flem, *J. Solid State Chem.* **22,** 121 (1977).
36. V. A. Cherepanov, L. Yu. Barkhatova, and A. N. Petrov, *J. Phys. Chem. Solids* **55,** 229 (1994).
37. P. Kofstad and A. Petrov, *in* "Proceedings, 14th Riso International Symposium on Materials Science: High Temperature Electrochemical Behaviour of Fast Ion and Mixed Conductors" (F. W. Poulsen *et al*., Eds.), p. 287. Riso Natl. Lab., Roskilde, Denmark, 1993.